THERMAL FIELD MODELING FOR WELDING WITHOUT FILLER MATERIAL

Dumitru Titi CICIC[1], Corneliu RONTESCU[2], Cătălin AMZA[3], Diana POPESCU[4]

The main purpose of this paper is to find methods of evaluation for the thermal field resulted from cladding by welding, without filler material, on a 13CrMo4-5 base material, by using computer solutions. The paper presents the results obtained following the simulation and the real experiment, as well as quantitative and qualitative comparisons between them.

Keywords: welding, thermal field, heat, analysis

1. Introduction

The current trend in the field of welded products is to minimize or eliminate the time lost with preliminary tests for the approval of weld, respectively of welding technologies. One of the possible methods to achieve this goal is to simulate the real working conditions by using specialized software. The current research trends are trying to pre-establish the thermal history of the work pieces by using specialized software.

During TIG welding, the power source provides a voltage difference, U, between the tungsten electrode and the work piece, which supports the formation of the electric arc.

However, due to losses that occur as a result of convection and radiation in both the electrode and the arc, only a part of this power is really used to heat and melt the material. The ratio between the useful power and the total power is known as arc efficiency, denoted by ε. Thus, the actual heat input per unit of time can be expressed as:

$$Q = \varepsilon \cdot Q_a = \frac{U \cdot I}{v \cdot 1000} \cdot \varepsilon \quad \text{(J/mm)} \qquad (2)$$

where: U – arc voltage (V); I – welding current intensity (A); v – welding speed (mm/s), ε - efficiency of the heat transfer from the electric arc to the parts to be welded (for TIG ε=0.6, according to [1].

[1] Lecturer, Faculty I.M.S.T., University POLITEHNICA of Bucharest, email: dumitru.cicic@gmail.com
[2] Lecturer, Faculty I.M.S.T., University POLITEHNICA of Bucharest, email: corneluts@yahoo.com
[3]Senior Lecturer, Faculty I.M.S.T., University POLITEHNICA of Bucharest, email: acata1@amza.camis.pub.ro
[4] Lecturer , I.M.S.T., University POLITEHNICA of Bucharest, email: dian_popescu@yahoo.com

The heat input distribution of the TIG heat source was considered for modeling the welding process. The most frequently used heat source models for superficial distribution are finite Gaussian distribution on a radius r_a (fig. 1a) and - for volumetric distribution - the finite 3D Gaussian distribution on a double ellipsoid (fig. 1b)[2,3,4].

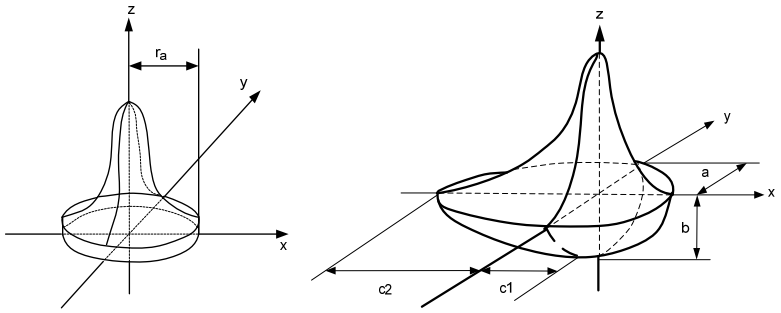

a) b)

Fig. 1 Gaussian heat source models: a) superficial distribution; b) volumetric distribution.

2. Experimental procedure

The simulation of the thermal field resulted during TIG welding by using two software packs was conducted starting from the following input data:

- base material: heat resistant low alloy steel 13CrMo4-5;
- dimensions of the model: 125 × 300 ×10 mm;
- the welding source is considered mobile and located in the middle of the plate;
- welding parameters for the real case: current I_s=216A, voltage U_a=15V, welding speed v_s=14cm/min.
- temperatures: the necessary temperatures for the build-up of the nodes of the created model are temperatures resulted from the thermographic examination; the general temperature of the created model is equal to the preheating temperature used during the experimental researches.

In order to show the distribution of temperatures in various spots on the surface of the analyzed plate we carried out the modeling of the thermal field with the help of Matlab program, a high performance interactive software pack, designed for mathematical, scientific and engineering calculations.

3. Obtained results

3.1. Modeling of the thermal field resulted during TIG welding by using Ansys software pack

The modeling process by finite element analysis was carried out with the help of Ansys program.

Modeling by finite element analysis creates the possibility to build new complex models both considering the geometry of the analyzed structure and considering the build-ups supported by the model. Modeling takes into account the thermal conduction, free or forced convection, the limit conditions concerning radiation, specific temperatures and the radiation rate on the surface or in volume.

Due to the nonlinear behavior during the welding process the chosen thermal analysis is transient and nonlinear.

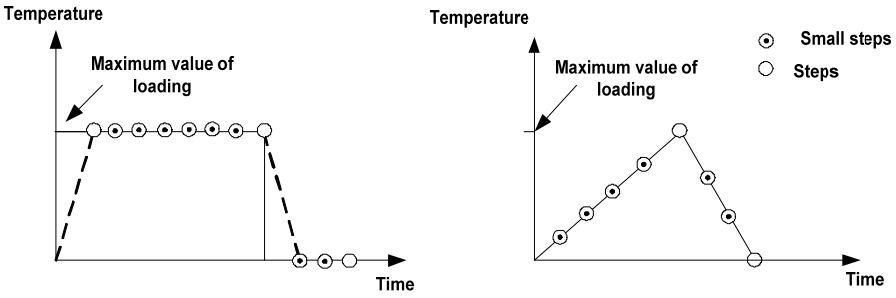

a) b)

Fig. 2. Load types of temperature depending on time
a) in steps; b) small steps in ramp

The transient thermal analysis is based on the same principle as thermal analysis of the equilibrium state, the main difference consisting of the fact that the build-up of the thermal analysis depends on time. This build-up - time dependence may be given either by defining an equation or by making a load curve depending on the time period defined in the form of build-up steps [5, 6].

For each build-up step both the value of the load and the time period, as well as the type of the load - in sub steps or ramp - should be indicated [7,8].

A nonlinear *transient* thermal analysis is carried out in order to highlight the aspects related to the solid-to-liquid phase change.

During the phase change analysis, there is a small temperature range within which both phases coexist. The finite element analysis will consider the latent heat occurring within the range between the two temperatures Tl (liquid phase temperature) and Ts (solid phase temperature).

For the transient analysis, the loads may vary with time, equation 2:

$$[C]\{\dot{T}\}+[K]\{T\}=\{Q(t)\} \tag{2}$$

where: [*C*] is the specific heat matrix;

[*T*] – derivative of temperature with respect to time;

[*Q*] – heat accumulated in the system;

[*K*] – heat conductivity matrix in time.

Where: for the nonlinear transient analysis with time and temperature:

$$[C(T)]\{\dot{T}\}+[K(T)]\{T\}=\{Q(T,t)\} \tag{3}$$

where: $[\mathrm{C(T)}]+\{T\}$ is calculated based on equation 4:

$$[\mathrm{C(T)}]+\{T\}=\int \rho c[N]^T[N]dV \tag{4}$$

where $[N]$ – temperature matrix depending on the heat flow.

During the experiments the welding source is considered mobile and located in the middle of the plates. The properties of the material are given depending on the material and are presented in table 1.

According to the input data presented in table 1, during the Preprocessor we carried out the plotting of the variations of conductivity and enthalpy depending on the temperature. The graphic variation of the material properties is presented in fig. 3.

Table 1

Values of the heat conductivity and heat content depending on time

Temperature [^{0}F]*	**Heat conductivity** [Btu/(hr·in·^{o}F)] *	**Heat content** [Btu/in^3]*
0	1.44	0
2643	1.54	128.1
2750	1.22	163.8
2875	1.22	174.2
3632	1.22	230.3
* - British units used in ANSYS analysis		

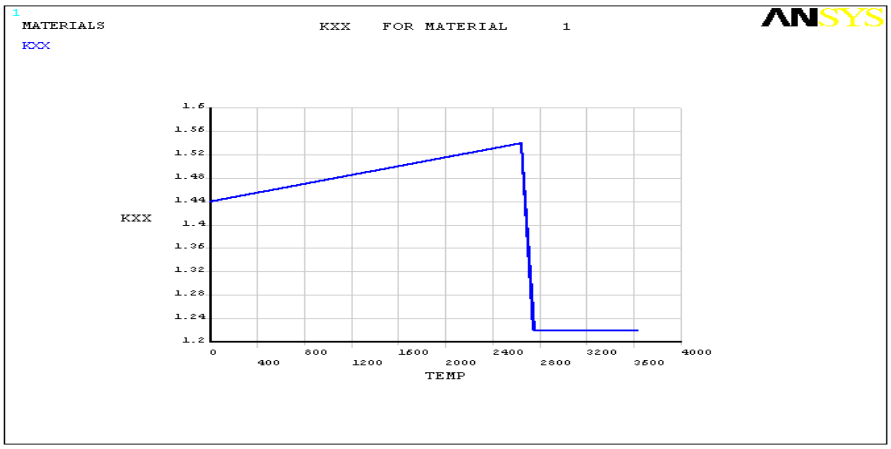

a)

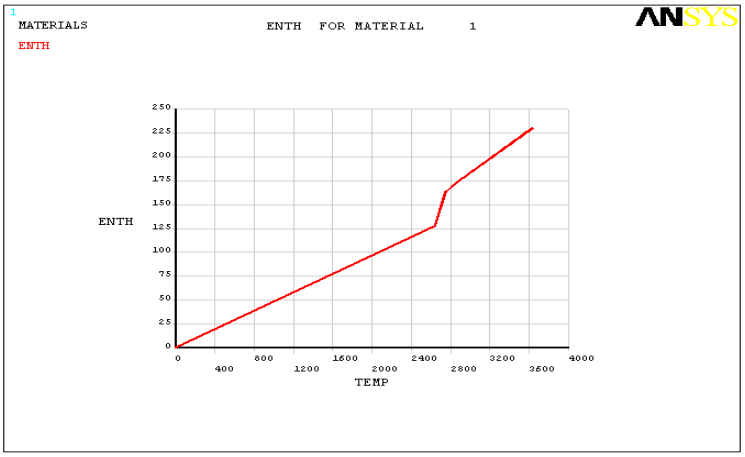

b)

Fig. 3. Graphic representation of the variation of conductivity (a) with heat content (b) with temperature

The element used in model meshing is SOLID 70, which is a 3D solid element with 3D thermal conduction capability. The model is discretized by splitting the lines corresponding to length *L5*, width *L8* and *L27* and thickness *L11*, so that the nodes on the movement line of the heat source can be distanced according to the welding speed and the time of the load step. The mesh was defined with hexahedral elements, dimensions 2.5x2.0x1.0 mm.

In order to have a line on the middle of the sample, *L5* in Figure 4, which should allow the selection of the nodes to be loaded with temperature, the total volume of the sample consists of two glued volumes.

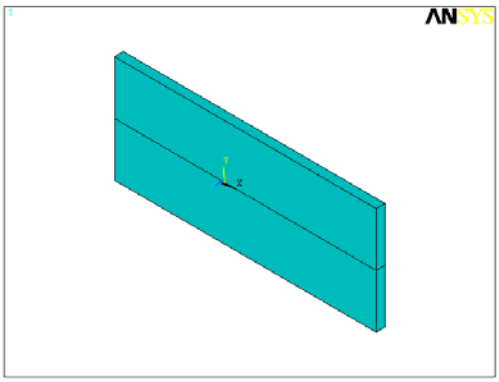

Fig. 4. Creating the volume

Solid70, a 3D element with thermal conduction capabilities, shown in Fig. 5, was chosen for discretization purposes from the elements library of Ansys**.**

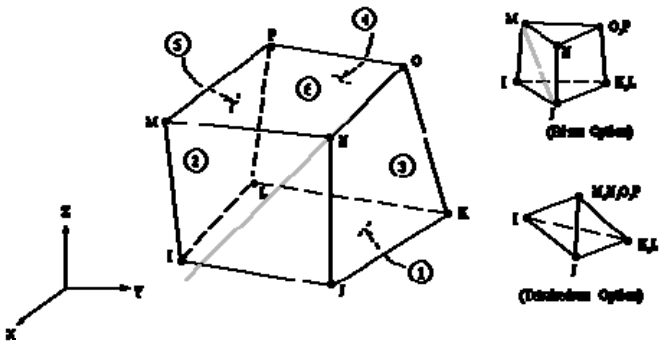

Fig. 5. Discretization element Solid70

In the nodes on the median line of the plate we applied temperature loads, from node 3757 corresponding to the arc ignition and further on the movement direction of the heat source (fig. 6). The temperature values applied to these nodes were determined by thermographic measurements.

Fig. 6. Discretization of the model and its load

3.2. Experimental results concerning the form of the weld pool and the form of the thermal field

Figs. 7 to 9 present the distribution of the temperature isotherms resulted at 15, 30 and 45 seconds from the beginning of the welding process in cross section along the weld pool and in isometric view.

As it happens during the TIG welding process, on the created model represented in cross section along the weld pool at 15 s from the arc ignition (fig. 7.a) the superheat in the end zone of the plate can be observed, and in the isometric view the non-stationary distribution of the thermal field can be observed (fig. 7.b.).

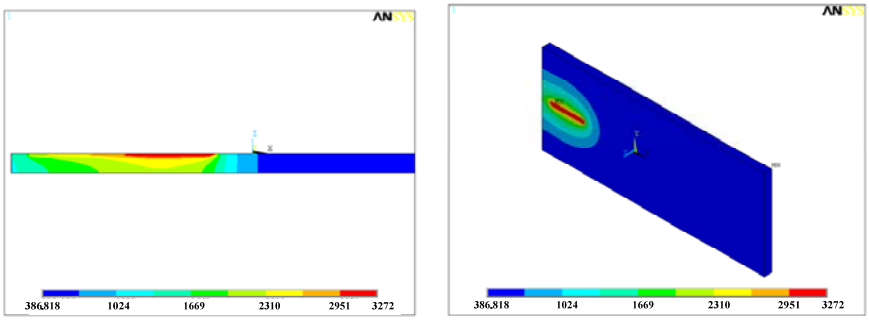

a) b)

Fig. 7. Cross section along the weld pool and isometric view of the isotherms at 15 seconds
a) cross section) b) isometric view

After 30 seconds the thermal field becomes quasi-stationary and behind the electric arc the weld pool cools off, and the melted metal takes the specific asymmetric semi-ellipsoidal shape (fig. 8).

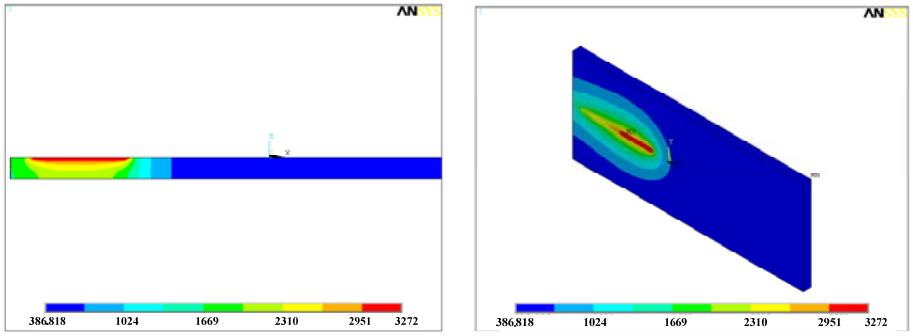

a) b)

Fig. 8. Cross section along the weld pool and isometric view of the isotherms at 30 seconds
a) cross section) b) isometric view

After 45 seconds the electric arc passes through more than half of the plate length, and in this area the analysis of the thermal field is carried out in cross section (fig. 9).

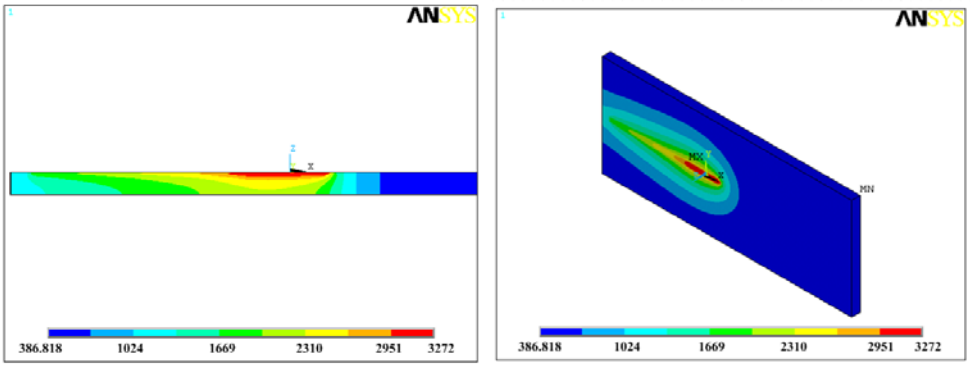

a) b)

Fig. 9. Cross section along the weld pool and isometric view of the isotherms at 45 seconds
a) cross section b) isometric view

3.3. Experimental results concerning the width, depth and variation of the thermal field

The cross section of the created model shows the two-dimensional model of heat propagation, also encountered during the practical researches.

The temperature distribution for two-dimensional propagation that resulted following the finite element simulation during the surface remelting on a plate by a single pass under the previously mentioned conditions is represented in figure 10.

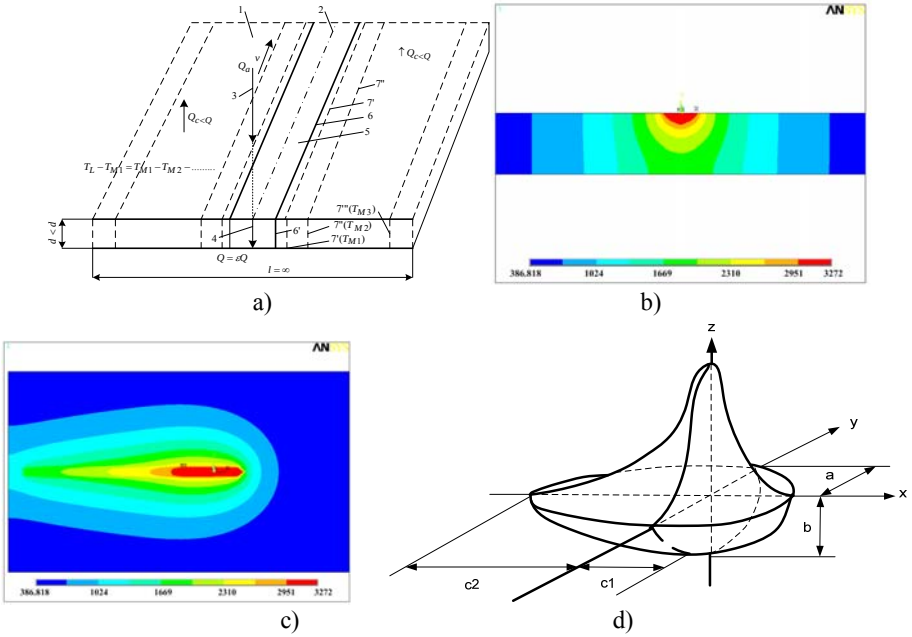

a) b)

c) d)

Fig. 10. Temperature distribution for two-dimensional heat propagation
a) theoretical model, b) cross section, c) front view d) theoretical model

We used the finite element analysis in order to obtain a model that presents the comparison between the images of transversal section of the weld pool obtained during the computational simulation (fig. 11.b) and the results obtained during the practical tests (fig 11.a), as well as the comparison between the width and penetration of the weld pool obtained both experimentally and by using the finite element analysis.

By analyzing figure 10 we can observe that there are differences between the results obtained following the simulation and the practical results; the model has the following errors:

- the error of the model resulted for the bead width amounts to 1.42%;
- the error of the model resulted for the penetration amounts to 1.56%.

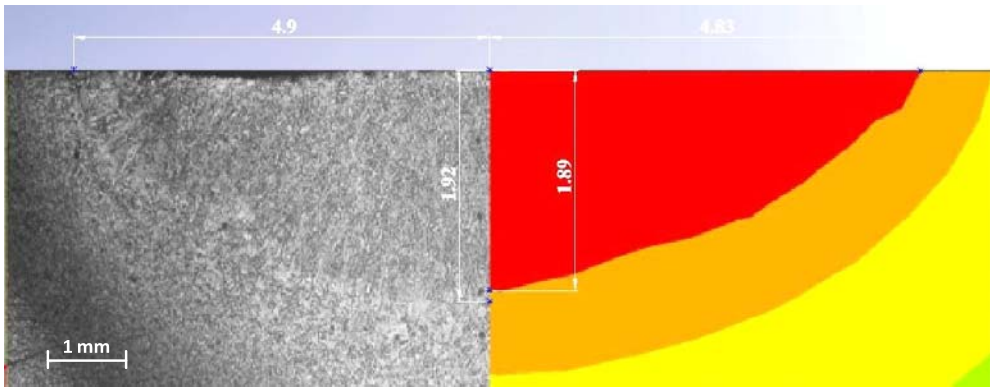

a) b)

Fig. 11 Comparison of macrographical images (experimental and simulation):
a) macrographical result obtained for the real sample b) cross section obtained following the simulation

5. Conclusions

1^0. The finite element modeling of the welding process and the analysis of figures 7-10 revealed that the heat distribution inside the sample occurs according to the Gaussian double ellipsoidal model;

2^0. The shape and dimensions of the weld pool resulted for the theoretical and the experimental model are the same;

3^0. By the finite element modeling the accuracy of the tridimensional distribution of the thermal field in the base material, as well as in the deposit was confirmed.

4^0. The results obtained following the transient thermal analysis, i.e. the thermal field distribution in various stages of the welding process and the geometrical elements of the bead, are similar to the experimental results, with an error range between 1.42 and 1.56%;

Acknowledgement

The work has been co-funded by the Sectorial Operational Programme Human Resources Development 2007-2013 of the Romanian Ministry of Labour, Family and Social Protection through the Financial Agreement POSDRU/89/1.5/S/62557.

R E F E R E N C E S

[1] *Gh. Solomon, Elemente* de teoria proceselor de sudare, Editura Bren, Bucuresti, 2001

[2] *X. H. Zhan*, Z. B. Dong, Y. H. Wei, and Y. L. Xu:* Dendritic grain growth simulation in weld molten pool based on ca-fd model, Cryst. Res. Technol. 43, No. 3, 253 – 259 (2008) / DOI 10.1002/crat.200710966

[3] *A.C. Bezerra, D. A. Rade, A. Scotti,* Simulation of a TIG Weld using Finite Element Method: Part 1 – Thermal Analysis, Soldagem Insp., Vol. 11, No. 1, Jan/Mar 2006

[4] *M. Cronje:* Finite element modeling of shielded metal arc welding, Thesis master of science, University of Stellenbosch, Matieland, South Africa, December 2005

[5] *D.K. Aidun, J.J. Domey, and G. Ahmadi:* Digital Simulations of a Stationary and a Linear Weld, Metallurgical and materials transactions, volume 33B, 2002—101

[6] *D. Berglunda, H. Albergb, H. Runnemalma:* Simulation of welding and stress relief heat treatment of an aero engine component, Finite Elements in Analysis and Design 39 (2003) 865–881

[7] *P.C. Zhao, C.S. Wu1, and Y.M. Zhang:* Modeling the transient behaviors of a fully penetrated gas–tungsten arc weld pool with surface deformation, Proc. IMechE Vol. 219 Part B: J. Engineering Manufacture, 2005

[8] *C. Schwenk*: *FE*-Simulation des Schweißverzugs laserstrahlgeschweißter dünner Bleche, Berlin, 2007